Manipulated localized surface plasmon resonances in silver nanoshells coated with a spherical anisotropic layer*

Jiang Shu-Min(蒋书敏)[a)], Wu Da-Jian(吴大建)[a)†], Cheng Ying(程 营)[b)], and Liu Xiao-Jun(刘晓峻)[b)‡]

[a)] *Faculty of Science, Jiangsu University, Zhenjiang* 212013, *China*
[b)] *School of Physics, Nanjing University, Nanjing* 210093, *China*

(Received 17 May 2012; revised manuscript received 7 June 2012)

The influences of the anisotropy of the outer spherically anisotropic (SA) layer on the far-field spectra and near-field enhancements of the silver nanoshells are investigated by using a modified Mie scattering theory. It is found that with the increase of the anisotropic value of the SA layer, the dipole resonance wavelength of the silver nanoshell first increases and then decreases, while the local field factor (LFF) reduces. With the decrease of SA layer thickness, the dipole wavelength of the silver nanoshell shows a distinct blue-shift. When the SA layer becomes very thin, the modulations of the anisotropy of the SA layer on the plasmon resonance energy and the near-field enhancement are weakened. We further find that the smaller anisotropic value of the SA layer is helpful for obtaining the larger near-field enhancement in the Ag nanoshell. The geometric average of the dielectric components of the SA layer has a stronger effect on the plasmon resonance energy of the silver nanoshell than on the near-field enhancement.

Keywords: Ag nanoshell, spherically anisotropic, Mie theory, localized surface plasmon resonance

PACS: 78.67.–n, 78.67.Bf, 36.40.Vz, 73.22.Lp **DOI:** 10.1088/1674-1056/21/12/127806

1. Introduction

Surface enhanced Raman scattering (SERS) based on metallic nanoparticles has attracted much attention because of its wide potential applications in chemical sensing, medical diagnostics, bioanalysis, and immunoassay.[1−3] The localized surface plasmon resonance (LSPR) in the metallic nanoparticles, originating from the collective oscillation of the conduction electrons in response to optical excitation, can induce a large local electromagnetic (EM) field near the surface of the nanoparticle.[4] Such an enlarged EM field is a key mechanism for the SERS and can enhance the Raman excitation and emission. Most of the solution-phase experiments in the SERS are performed using either Ag or Au nanoparticles. It is well known that the Ag nanoparticles show a 100–1000 times stronger Raman enhancement in comparison with that of the Au nanoparticles. However, the Ag nanoparticles have the disadvantages of instability and biotoxicity.[5] In order to overcome the disadvantages of both gold and silver nanoparticles, there have been many attempts to obtain core-shell particles, such as Ag/Au nanoshell,[6] three-layered Ag/Au nanoshell,[7] and Ag/Au alloy nanoshell.[8]

Recently, the composite nanostructures consisting of anisotropic materials and metal nanoparticles have also been widely studied because of their applications in optical devices, SERS, and optical nonlinearity enhancement. For example, Park and Stroud[9] have found that the optical properties of the gold nanoparticles coated with the anisotropic nematic liquid crystal can be controlled by a static electric field. The adjustment of the dielectric anisotropy in the core or shell may result in large enhancements of both second harmonic generation and induced third harmonic generation susceptibilities at surface plasmon resonant frequencies.[10] Yin *et al.*[11] have investigated the SERS enhancement from a coated nanosphere with a

*Project supported by the National Basic Research Program of China (Grant No. 2012CB921504), the National Natural Science Foundation of China (Grant Nos. 10904052, 11174113, and 11104319), the Jiangsu Planned Projects for Postdoctoral Research Funds, China (Grant No. 1002075C), and the Senior Talent Foundation of Jiangsu University, China (Grant No. 09JDG073).

†Corresponding author. E-mail: wudajian@ujs.edu.cn
‡Corresponding author. E-mail: liuxiaojun@nju.edu.cn

© 2012 Chinese Physical Society and IOP Publishing Ltd

spherical anisotropy shell, and found that the introduction of spherical anisotropy into the shell provides a novel approach to tailoring the surface plasmon resonant frequencies and enhancing the SERS peaks. It is further found that the large anisotropy shell can enhance the electric field in the core region, which will drive an enhanced nonlinear response.[12] However, a spherically anisotropic shell-coated metal nanosphere possesses an LSPR in the visible region, which will be an impediment to their biomedical applications.

In this paper, we propose a spherically anisotropic (SA) layer-coated silver nanoshell (D–Ag–SA). The outer SA layer may protect the oxygen-free Ag in air and prevent Ag from ionizing in aqueous solution. The extinction spectra and near-field distributions of the D–Ag–SA nanoshells are calculated by using a modified Mie scattering theory. It is found that the decrease of the Ag shell thickness can easily move the LSPR of the D–Ag–SA nanoshell from the visible region into the near infrared region. We further investigate the effects of the anisotropy, thickness, and geometric average of dielectric components of the outer SA layer on the far-field spectrum and near-field enhancement of the D–Ag–SA nanoshell.

2. Electromagnetic scattering model

The composite nanoshell consists of a particle with a dielectric core of radius r_1, a middle silver shell of radius r_2, and an outer SA layer of radius r_3. The dielectric constants of the inner core, middle shell, outer layer, and embedding medium are ε_1, ε_2, ε_3, and ε_4, respectively. The specific geometry of a D–Ag–SA nanoshell is shown in Fig. 1.

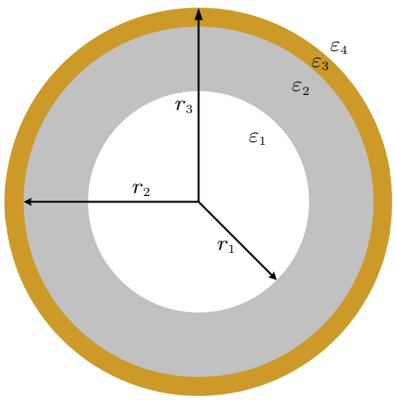


Fig. 1. (colour online) Geometry diagram of a D–Ag–SA nanoshell.

The outer SA layer is characterized by constitutive tensors of permittivity

$$\overleftrightarrow{\varepsilon}_3 = \begin{pmatrix} \varepsilon_{3r} & 0 & 0 \\ 0 & \varepsilon_{3t} & 0 \\ 0 & 0 & \varepsilon_{3t} \end{pmatrix}, \tag{1}$$

where the identity dyadic $\overleftrightarrow{I} = \hat{r}\hat{r} + \hat{\theta}\hat{\theta} + \hat{\phi}\hat{\phi}$. In the middle Ag shell, ε_2 has real and imaginary frequency-dependent components, and the dielectric function should be affected by the scattering of the conduction electrons in the particle surface. Thus, ε_2 is usually accounted by replacing the ideal Drude part in the dielectric function with a size-dependent one, and can be expressed as[13]

$$\varepsilon_2 = 1 - \frac{\omega_{\rm p}^2}{\omega^2 + {\rm i}\omega\gamma} + \chi_\infty, \tag{2}$$

where the background susceptibility χ_∞ arises from the core electron polarizability and interband transition, $\omega_{\rm p}$ is the bulk plasma frequency, and γ is the modified collision frequency and can be expressed as

$$\gamma = \gamma_{\rm f} + A\frac{V_{\rm f}}{a}, \tag{3}$$

with $\gamma_{\rm f}$ being the bulk collision frequency, $V_{\rm f}$ being the Fermi velocity, and the reduced electron mean free path a equates to the Ag shell thickness $(r_2 - r_1)$. For simple Drude theory and isotropic scattering, $A = 1$.[13] The bulk collision frequency for Ag is 3.2258×10^{13} s^{-1}, and the Fermi velocity for Ag is 1.39×10^6 m/s.[14] The parameters can be obtained by fitting the dielectric function to a particular frequency range of bulk dielectric data for Ag.[14] Throughout the paper, the inner dielectric core is assumed to be SiO_2 core. Thus, ε_1 is fixed at 2.04.

Light scattering by a spherical particle can be expressed through Debye potentials.[15] For spherically anisotropic material, the electric $\psi_{\rm TM}$ and magnetic $\psi_{\rm TE}$ Debye potentials are presented as[16]

$$\frac{\varepsilon_r}{\varepsilon_t}\frac{\partial^2\psi_{\rm TM}}{\partial r^2} + \frac{1}{r^2\sin\theta}\frac{\partial}{\partial\theta}\left(\sin\theta\frac{\partial\psi_{\rm TM}}{\partial\theta}\right) + \frac{1}{r^2\sin^2\theta}\frac{\partial^2\psi_{\rm TM}}{\partial\varphi^2} + k_0^2\varepsilon_r\mu\psi_{\rm TM} = 0, \tag{4}$$

$$\frac{\partial^2\psi_{\rm TE}}{\partial r^2} + \frac{1}{r^2\sin\theta}\frac{\partial}{\partial\theta}\left(\sin\theta\frac{\partial\psi_{\rm TE}}{\partial\theta}\right) + \frac{1}{r^2\sin^2\theta}\frac{\partial^2\psi_{\rm TE}}{\partial\varphi^2} + k_0^2\varepsilon_t\mu\psi_{\rm TE} = 0. \tag{5}$$

Here, $k_0 = 2\pi/\lambda$ is the wave vector in a vacuum and μ is assumed to be 1. For isotropic material, $\varepsilon_r = \varepsilon_t$.

The electromagnetic waves are expanded to spherical partial waves by using vector spherical harmonics, and then Maxwell's boundary conditions are used to resolve the unknown expansion coefficients of the scattered and interior waves. According to the Mie scattering theory, the obtained extinction efficiency $Q_{\rm ext}$, scattering efficiency $Q_{\rm sca}$, and absorption efficiency $Q_{\rm abs}$ can be expressed as[15]

$$Q_{\rm ext} = \frac{2}{(k_4 r_3)^2} \sum_{n=1}^{\infty} (2n+1) {\rm Re}(a_n + b_n), \quad (6)$$

$$Q_{\rm sca} = \frac{2}{(k_4 r_3)^2} \sum_{n=1}^{\infty} (2n+1)(|a_n|^2 + |b_n|^2), \quad (7)$$

$$Q_{\rm abs} = Q_{\rm ext} - Q_{\rm sca}. \quad (8)$$

The quantities a_n and b_n are the scattering coefficients, and Re means the real part. The information about the spherically anisotropic outer shell is presented by the order of spherical Bessel functions[16]

$$v = \left[n\,(n+1)\,\frac{\varepsilon_{3t}}{\varepsilon_{3r}} + \frac{1}{4} \right]^{1/2} - \frac{1}{2}. \quad (9)$$

3. Results and discussion

In Fig. 2, the solid line represents the absorption spectrum of the D–Ag–SA nanoshell with geometry of [45-50-55-7-1]. Here, [45-50-55-7-1] means $r_1 = 45$ nm, $r_2 = 50$ nm, $r_3 = 55$ nm, $\varepsilon_i = 7$, and $\rho = 1$ for the D–Ag–SA nanoshell. We assume the anisotropic value $\varepsilon_{3t}/\varepsilon_{3r}$ to be ρ. In order to clarify the role of anisotropy, we keep the geometric average of the dielectric components $\varepsilon_i = \varepsilon_{3r}/3 + 2\varepsilon_{3t}/3$ unchanged for the SA layer,[11,12] while ρ-value is varied. In the solid line, the strong peak appears at ~ 930 nm, which arises from the dipole plasmon resonance. At the shoulder of the dipole peak, the quadrupole resonance peak appears at ~ 735 nm. The dotted, dash–dot, dash–dot–dot, and short–dash lines present the absorption spectra of the D–Ag–SA nanoshells with [45-50-55-7-5], [40-50-55-7-5], [45-50-51-7-5], and [45-50-55-10-5], respectively. It is obvious that the decrease of Ag layer thickness can lead to a large red-shift of the LSPR. The anisotropy, thickness and ε_i-value of the SA layer all significantly affect the LSPR properties of the D–Ag–SA nanoshells.

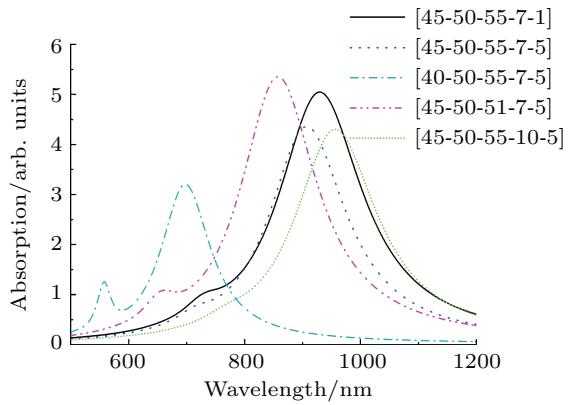


Fig. 2. (colour online) Absorption spectra of the D–Ag–SA nanoshells with various [r_1-r_2-r_3-ε_i-ρ].

We first discuss the influences of the anisotropy and ε_i-value of the outer SA layer on the far-field spectra. In Fig. 3, the circle-dash line shows the dependence of the dipole resonance wavelength of the D–Ag–SA nanoshell on the ρ-value. Here, the radii of inner core, Ag layer, and outer shell are fixed at 45, 50, and 55 nm, respectively. The value of ε_i is fixed at 7. It is found that with the increase of ρ-value, the dipole plasmon resonance of the D–Ag–SA nanoshell first increases from 893 nm at $\rho = 1/10$ to 930 nm at $\rho = 1$ and then decreases to 867 nm at $\rho = 10$. The LSPR of the D–Ag–SA nanoshell can be known as the hybridization between a dipolar cavity plasmon on the inner surface (ω_c) and a plasmon of the particle consisting of a solid Ag sphere coated by an SA layer (ω_s).[17,18] The hybridization between ω_c and ω_s will lead to two new resonance modes. The low energy mode ω_- corresponds to a symmetric coupling between ω_c and ω_s, and the high energy mode ω_+ corresponds to an antisymmetric coupling. The variations of the permittivity of the SA layer only lead to the change in ω_s mode. The red-shift of the ω_- dipole mode means the plasmon energy of the ω_s mode reducing, which arises from the decrease of the induced charges in the outer surface of the Ag layer.[19] Contrarily, the increase of the induced charges in the outer surface of the Ag layer happens. The square–dash, triangle–dash, and star–dash lines show the variations for $\varepsilon_i = 4$, 10, and 15, respectively. With the increase of ε_i-value, the dipole wavelength of the D–Ag–SA nanoshell shows a red-shift at each ρ-value. This is because the increase of ε_i-value will lead to the decrease of the induced charges in the outer surface of the Ag layer and hence the resonance energy of the ω_- mode decreases. We further find that, when $\rho < 1$, the D–Ag–SA nanoshell with the larger ε_i-value exhibits the larger red-shift of the dipole plasmon wavelength with ρ-value increasing. When $\rho > 1$, the larger blue-shift of the dipole wavelength happens in the particle

with the smaller ε_i-value.

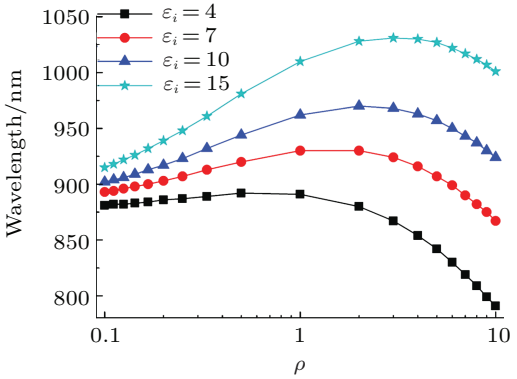


Fig. 3. (colour online) Dependencies of the dipole resonance wavelength for D–Ag–SA nanoshells with various ε_i-values and ρ-values. Here, $r_1 = 45$ nm, $r_2 = 50$ nm, $r_3 = 55$ nm.

Figure 4 shows the dependencies of the dipole wavelength of the D–Ag–SA nanoshell on ρ-value. The square–dash, circle–dash, triangle–dash, and star–dash lines show the variations for the D–Ag–SA nanoshells with SA layer radii of 55, 52, 51, and 50.5 nm, respectively. Here, r_1, r_2, and ε_i are fixed at 45 nm, 50 nm, and 7, respectively. It is found that for each SA layer thickness, the dipole wavelength of the D–Ag–SA nanoshell always first increases and then decreases with ρ-value increasing. For each ρ-value, the larger thickness of outer SA layer will always lead to the longer wavelength for the dipole mode. Yan *et al.*[20] have reported that with the increase of the dielectric shell thickness, the plasmon resonance energy of the dielectric coated metal nanosphere will be reduced. Thus, the increased thickness of the SA layer will cause the reduced plasmon energy of the ω_s mode and hence the decreased energy of the ω_- mode. In addition, the larger thickness of the SA layer leads to the stronger variation of the LSPR for the D–Ag–SA nanoshell with ρ-value.

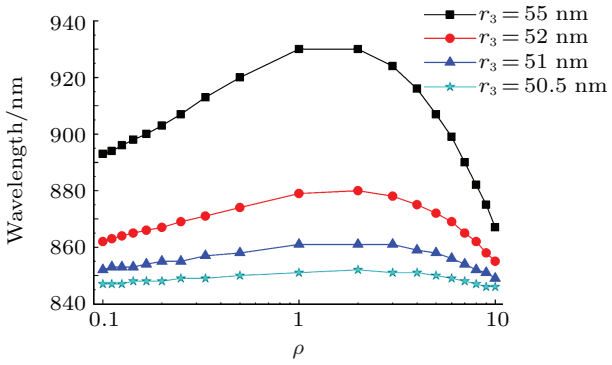


Fig. 4. (colour online) Dependencies of the dipole resonance wavelength for D–Ag–SA nanoshells with various r_3-values and ρ-values. Here, $r_1 = 45$ nm, $r_2 = 50$ nm, $\rho = 7$.

Figures 5(a)–5(c) show the E-field enhancement distributions of D–Ag–SA nanoshells with $\rho = 1$, $\rho = 1/5$, and $\rho = 5$, respectively, which are calculated at the dipole resonance wavelengths of 903, 930, and 907 nm. Here, $r_1 = 45$ nm, $r_2 = 50$ nm, $r_3 = 55$ nm, and $\varepsilon_i = 7$. The incident polarization is along the y axis. In Fig. 5(a), the large electric field (E-field) is located within a few nm of the shell surface and occurs along the incident polarization, which arises from the dipole plasmon resonance.[21] The field lines inside the middle Ag layer repel each other in the poles along the incident polarization and bunch at the poles perpendicular to the polarization direction, which is due to the fact that the electrons of the same kind are induced on the inner and outer surfaces of the Ag layer.[22] The weak E-field in the outer shell is due to the larger dielectric constant. The similar E-field distributions have been found in the D–Ag–SA nanoshells with $\rho = 1/5$ and $\rho = 5$. The variation of ρ-value will lead to a different enhancement of E-field in the D–Ag–SA nanoshell. Figure 4(d) shows the variation of the E-field enhancement along y-axis. The solid, dashed, and dotted lines show the variations of E-field enhancement in the nanoshells with $\rho = 1$, $\rho = 1/5$, and $\rho = 5$, respectively. The smaller ρ-value will cause the larger enhancement of E-field, which can be found outside the particle, inside the SA shell, and inside the core separately. The E-field enhancement inside the SA layer is more sensitive to the variation of ρ-value.

Finally, we investigate the influences of the anisotropy, thickness, and ε_i-value of the outer SA layer on the near-field enhancement of the D–Ag–SA nanoshell. In Fig. 6, the circle–dash line shows the dependence of the local field factor (LFF) of the D–Ag–SA nanoshell on ρ-value. Here, the radii of the inner core, Ag layer, and outer shell are fixed at 45, 50, and 55 nm, respectively. The value of ε_i is fixed at 7. We assume the maximum of the near-field enhancement $|\boldsymbol{E}/\boldsymbol{E}_{\rm in}|_{\rm max}$ at dipole resonance wavelength to be the LFF, which is located on the outer surface of the particle and at the poles along the incident polarization. It is found that with the increase of ρ-value the LFF of the D–Ag–SA nanoshell decreases considerably. The similar decreases of LFF can also be observed in the D–Ag–SA nanoshell with $\varepsilon_i = 4$ (square–dash line), $\varepsilon_i = 10$ (triangle–dash line), and $\varepsilon_i = 15$ (star–dash line). However, the effect of the variation of ε_i on the near-field enhancement of the D–Ag–SA nanoshell is weak.

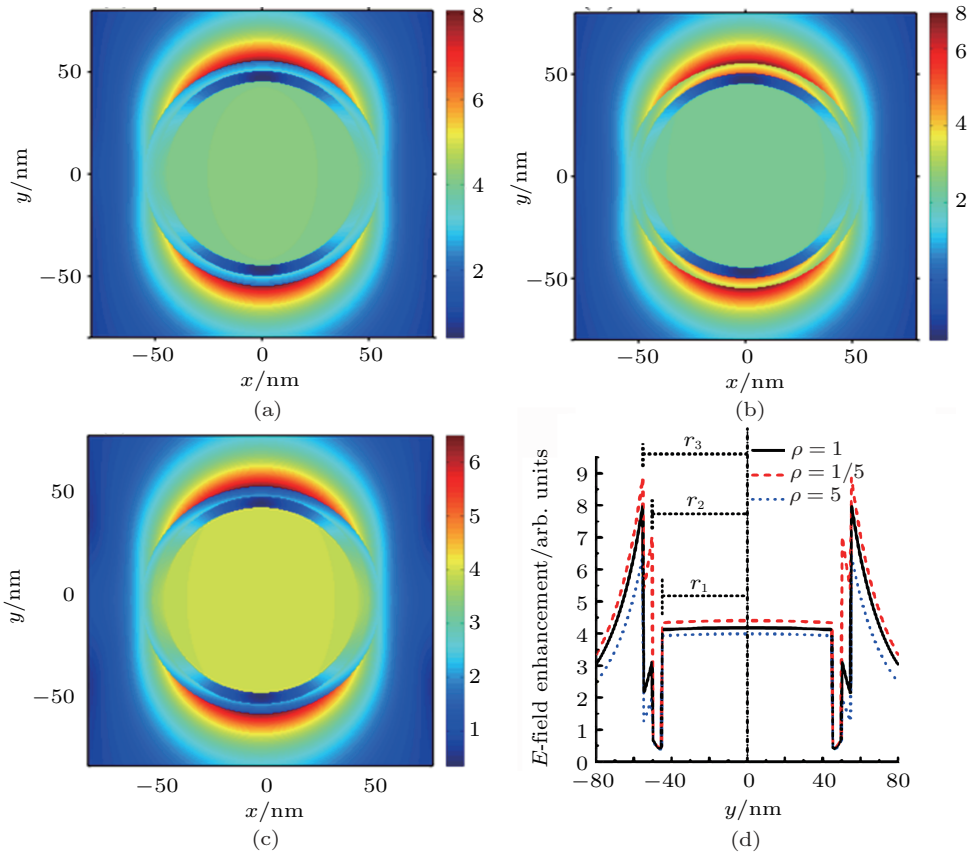


Fig. 5. (colour online) Electric field enhancement distributions of D–Ag–SA nanoshell with (a) $\rho = 1$, (b) $\rho = 1/5$, and (c) $\rho = 5$. (d) Variation of E-field enhancement along y axis. Here, $r_1 = 45$ nm, $r_2 = 50$ nm, $r_3 = 55$ nm, and $\varepsilon_i = 7$.

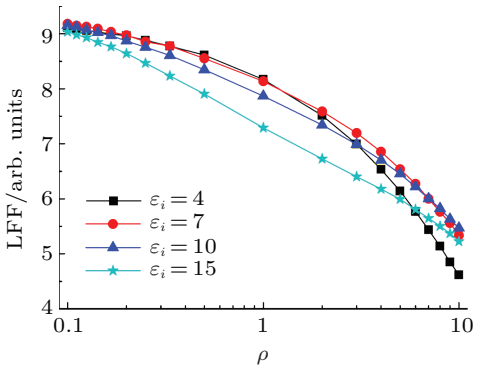


Fig. 6. (colour online) Dependencies of LFF for D–Ag–SA nanoshells with various ε_i-values and ρ-values. Here, $r_1 = 45$ nm, $r_2 = 50$ nm, $r_3 = 55$ nm.

In Fig. 7, the square–dash line shows the dependence of the LFF of the D–Ag–SA nanoshell on ρ-value. Here, $r_1 = 45$ nm, $r_2 = 50$ nm, $r_3 = 55$ nm, and $\varepsilon_i = 7$. It is found that with the increase of ρ-value the LFF of the D–Ag–SA nanoshell decreases from 9.181 at $\rho = 1/10$ to 5.337 at $\rho = 10$. For different radii of the SA shell, the LFF of the D–Ag–SA nanoshell always decreases with the increase of ρ-value. However, the variation of the LFF in the D–Ag–SA nanoshell with a thin SA layer is weaker than, in particular, with a thick SA layer. When $r_3 = 50.5$ nm, with ρ-value increasing, the LFF only decreases from 9.706 at $\rho = 1/10$ to 9.223 at $\rho = 10$. In addition, for each ρ-value, the smaller thickness of the outer SA layer will lead to the larger LFF of the D–Ag–SA nanoshell. This is because the decreased thickness of the SA layer will reduce the separation between the Ag layer and the outer surface. In this case, the effects of the induced charges in the inner and outer surfaces of the Ag layer on the near field are enhanced, thereby enhancing the LFF.

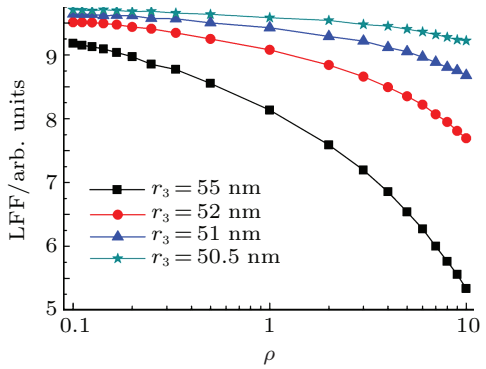


Fig. 7. (colour online) Dependencies of the LFF for D–Ag–SA nanoshells with various r_3-values and ρ-values. Here, $r_1 = 45$ nm, $r_2 = 50$ nm, $\varepsilon_i = 7$.

4. Conclusions

We investigated the far- and near-field properties of the D–Ag–SA nanoshells by Mie scattering theory. With the increase of anisotropic value of the SA layer, the dipole resonance wavelength of the D–Ag–SA nanoshell first increases and then decreases while the near-field enhancement is reduced. The increased ε_i-value leads to a distinct red-shift of the plasmon resonance energy in the D–Ag–SA nanoshell. We further found that the smaller thickness of the SA layer leads to the larger plasmon energy and larger near-field enhancement in the D–Ag–SA nanoshell. Therefore, the SA shell can easily manipulate LSPR properties in D–Ag–SA nanoshells, and the large near-field enhancement in near-infrared region should be obtained, which may be useful for the further applications in the SERS and the optical devices.

References

[1] Potara M, Baia M, Farcau C and Astilean S 2012 *Nanotechnology* **23** 055501

[2] Hu J and Zhang C Y 2012 *Biosensors & Bioelectronics* **31** 451

[3] Lee S, Chon H, Yoon S Y, Lee E K, Chang S I, Lim D W and Choo J 2012 *Nanoscale* **4** 124

[4] Kreibig U and Vollmer M 1995 *Optical Properties of Metal Clusters* (Berlin: Springer)

[5] Laserna J J 1993 *Anal. Chem. Acta* **283** 607

[6] Cui Y, Ren B, Yao J L, Gu R A and Tian Z Q 2006 *J. Phys. Chem.* B **110** 4002

[7] Wu D J and Liu X J 2010 *Appl. Phys. Lett.* **96** 151912

[8] Wu D J and Liu X J 2010 *Appl. Phys. Lett.* **97** 061904

[9] Park S Y and Stroud D 2005 *Phys. Rev. Lett.* **94** 217401

[10] Gao L and Yu X P 2007 *Eur. Phys. J.* B **55** 403

[11] Yin Y D, Gao L and Qiu C W 2011 *J. Phys. Chem.* C **115** 8893

[12] Liu D H, Xu C and Hui P M 2008 *Appl. Phys. Lett.* **92** 181901

[13] Averitt R D, Westcott S L and Halas N J 1999 *J. Opt. Soc. Am.* B **16** 1824

[14] Johnson P B and Christy R W 1972 *Phys. Rev.* B **6** 4370

[15] Bohren C F and Huffman D R 1983 *Absorption and Scattering of Light by Small Particles* (New York: Wiley)

[16] Luk'yanchuk B S and Qiu C W 2008 *Appl. Phys.* A **92** 773

[17] Prodan E, Radloof C, Halas N J and Nordlander P 2003 *Science* **302** 419

[18] Wu D J and Liu X J 2011 *Appl. Phys.* A **105** 439

[19] Prodan E, Lee A and Nordlander P 2002 *Chem. Phys. Lett.* **360** 325

[20] Yan S N, Wang Y C, Wen T D and Zhu J 2006 *Physica* E **33** 139

[21] Kelly K, Coronado E, Zhao L L and Schatz G C 2003 *J. Phys. Chem.* B **107** 668

[22] Prodan E and Nordlander P 2004 *J. Chem. Phys.* **120** 5444